Available online at www.sciencedirect.com
ScienceDirect
Journal of Sound and Vibration 318 (2008) 663–677
JOURNAL OF SOUND AND VIBRATION
www.elsevier.com/locate/jsvi

Extremal harmonic active control of power for rotating machines

Jean-Philippe Gauthier*, Philippe Micheau

G.A.U.S. (Groupe d'Acoustique de l'Universite de Sherbrooke), 2500 Boulevard Universite, Sherbrooke, Quebec, Canada J1K2R1

Received 15 October 2007; received in revised form 22 April 2008; accepted 23 April 2008
Handling Editor: S. Bolton
Available online 9 June 2008

Abstract

Most of the time, the speed of rotating machines oscillates in synchronization with the rotor position. Those speed fluctuations, generated by disturbance torques, can be actively controlled with a second torque source coupled to the shaft of the machine. To achieve this active control, the problem is reformulated in the harmonic domain with regard to the main order of the fluctuations. The control objective is to extremalize an energetic criterion like kinetic energy (cancelling the speed ripple), reactive power (to add a virtual flywheel) or active power (to charge a battery). To reach those objectives, two extremal controllers are proposed with implicit or explicit criterion management. The controllers are tested on an academic test bed. The results show that the controllers converge at the extremum of each criterion.

1. Introduction

Rotating systems often create vibrations. If a system is well balanced, those vibrations are mostly created by periodic torque ripple which is synchronized with the rotating shaft position. For example, the combustion engine of a parallel hybrid vehicle drivetrain will make a fluctuating torque with a frequency that is dependant to crankshaft position and the number of cylinders [1]. A peristaltic pump is another example of a rotating machine with fluctuating torque involved [2]. Those torques create excessive wear and fatigue to the couplings and gearboxes of those systems. Also, it creates low frequency vibrations and noise which is difficult to damp with classical acoustic materials. Finally, the periodic speed fluctuation created by the torque ripple can affect negatively the process achieved by the rotating machine. For example, a wind turbine generator will add unwanted disturbances to the power grid [3].

Those speed fluctuations, generated by disturbance torques, can be actively controlled with a second torque source coupled to the shaft of the machine [4]. This second torque source has to deliver precise torque at different frequencies. With the help of a modern servo-amplifier, the electric motor delivers precise torque at high frequencies. All previous works, made to control the torque ripple of rotating machines, use an electric motor as the commanded torque source [1,5–11]. Those works have been concentrated on torque ripple

*Corresponding author. Tel.: +1 819 821 7657x 66073.
E-mail address: jeanphilippeg@gmail.com (J.-P. Gauthier).

0022-460X/$ - see front matter © 2008 Elsevier Ltd. All rights reserved.
doi:10.1016/j.jsv.2008.04.049

Nomenclature

α	losses coefficient
b	viscous damping coefficient (N s/rad)
f_c	cutoff frequency of the mechanical system
H	transfer function phasor of the mechanical system at first order
I	moment of inertia (kg m^2)
k	sample number
k_e	electric motor torque constant (N m/A) ($\tau = k_e i$)
μ	converging coefficient of the controller
n	order number
N	mean rotating speed (rev/min)
ω_c	cutoff frequency of the mechanical system (rad/s)
ω_n	frequency at the order n (rad/s)
Q_n	criterion to optimize with the controller
R	electric motor winding resistance (Ω)
τ	instantaneous commanded torque (N m)
τ_d	instantaneous disturbance torque (N m)
θ	shaft angle (rad)
$\dot{\theta}$	instantaneous rotation speed (rad/s)
$\dot{\theta}_0$	instantaneous rotation speed when $\tau = 0$ (rad/s)
T	commanded torque phasor (N m)
T_d	disturbance torque phasor (N m)
T_{opt}	optimal commanded torque phasor (N m)
W	rotation speed phasor (rad/s)
W_0	rotation speed phasor without active control (rad/s)
Y	mechanical admittance of the system

created by combustion engines in vehicles. The approach presented in this paper is more general to allow torque ripple control to be used with any fluctuating torque system.

To achieve active control, torque observers were used to characterize the torque ripple of a combustion engine [1,5]. Knowing the instantaneous torque of the engine, the controller can then set the secondary torque to cancel the fluctuating part of the engine torque. This strategy needs a highly complex observer, especially configured to fit a particular engine. This worsens the portability of the algorithm. Other works have been concentrated on observer synthesis [6]. In those cases, the best observer architecture has been developed to fit the particular situation of instantaneous torque ripple control. The observer is then used like in the first case to cancel torque ripple. A simpler approach used open loop periodic control [7]. With the help of an angle sensor, a predefined torque was added to the system by a secondary torque source. The results showed that creating a counter torque to oppose the fluctuating torque helps reduce the torque ripple. But, the secondary torque source being underpowered, the results were marginal. Digital filters [8,9] were used also to control torque ripple. The main speed fluctuation signal is isolated by a notch filter, then the secondary torque is created by using this speed signal and the system inertia. Finally, adaptive controllers using Fourier coefficients have been proposed [10,11]. In this case, one or more Fourier coefficients are combined to create a periodic fluctuating secondary torque. With an adaptive control strategy, the optimal amplitude and phase is obtained and torque ripple can be cancelled.

Each of these control strategies try to cancel either the torque ripple or the speed ripple of the mechanical system without considering the power characteristics of the control. As of today, very few experimental results or studies on power consumption were published. Knowing the energetic requirements of a given control strategy is necessary because it informs about the cost to control according to this strategy. Another problem is that each controller have to be specifically adapted for a given rotative system; this made the instantaneous torque control a solution that is still not used in practical applications. The goal of this article is to propose a kind of controller that works without modification on any rotating machine with a periodic torque fluctuation. Also, the energetic requirements of the control strategy will be checked, being aware that high power consumption will have a negative effect on the efficiency of the given machine.

The first part of this study is to theoretically modelize the problem of active control in rotating machines as an electrical problem of controlling active or reactive power. Hence, based on the behavior of the electrical model, three types of energetical criterions are proposed, each of them achieving a different goal. Whatever is the criterion, an extremal controller can be used to reach the extremum value of the said criterion. Two extremal controllers are proposed with implicit or explicit criterion management. Finally, an experimental setup has been used and the results of it describes well the converging pattern of each controller.

2. Mechanical configuration

The typical problem addressed in this work is presented in Fig. 1. The studied system is a rotating machine which creates a disturbance torque τ_d on a shaft (e.g. combustion engine). Coupled to the shaft, a variable torque source (an electric motor) is commanded by a control algorithm to supply a fluctuating anti-torque τ. The load, in Fig. 1, gathers the mechanical dynamics of all the moving parts.

The input of the system is the torque τ and the output is the rotating speed $\dot{\theta}$. The complete system can be modelized in Laplace domain:

$$\dot{\theta}(s) = Y(s)\tau(s) + \dot{\theta}_0(s), \tag{1}$$

where $\dot{\theta}(s)$ is the instantaneous rotating speed, $\dot{\theta}_0(s) = Y(s)\tau_d(s)$ the rotating speed without active control (when $\tau(s) = 0$) and $\tau(s)$ the commanded torque. $Y(s)$ is the mechanical admittance of the system [12] (e.g. the load in Fig. 1). For example, the special case of a load constituted of an inertia I and a viscous damping b, the mechanical admittance is

$$Y(s) = \frac{1/b}{(I/b)s + 1}. \tag{2}$$

Referring to Eq. (2), the system can be approximated as $Y(s) \cong 1/b$ at low frequencies ($f \ll f_c$) and $Y(s) \cong 1/Is$ at high frequencies ($f \gg f_c$), $f_c = b/2\pi I$ being the cutoff frequency.

2.1. Order model

To achieve the active control, the problem is reformulated in the harmonic domain with regards to the main order of the speed fluctuations. The harmonic order n is the integral number defined by the ratio of the order frequency to the fundamental frequency of the fluctuating speed [13]. Hence, the frequency of an order n can be defined as

$$\omega = \frac{2\pi}{60} Nn, \tag{3}$$

where N is the mean shaft speed in revolutions per minute. Since torques and speeds respect the superposition principle, the order model allows the control of a disturbance torque made of several orders [10]. In this study, without loss of generality, the control of the main order of the signals is considered. For the rotating speed, the phasor of any order n is computed by integrating the instantaneous rotating speed $\dot{\theta}$ multiplied by $e^{-j\theta n}$ over a complete rotation of the shaft angle θ:

$$W = \frac{1}{\pi} \int_0^{2\pi} \dot{\theta}(\theta) e^{-j\theta n} \, d\theta. \tag{4}$$

The fluctuating commanded torque is generated as a function of the torque phasor T as

$$\tau(\theta) = \mathrm{Re}[T e^{j\theta n}], \tag{5}$$

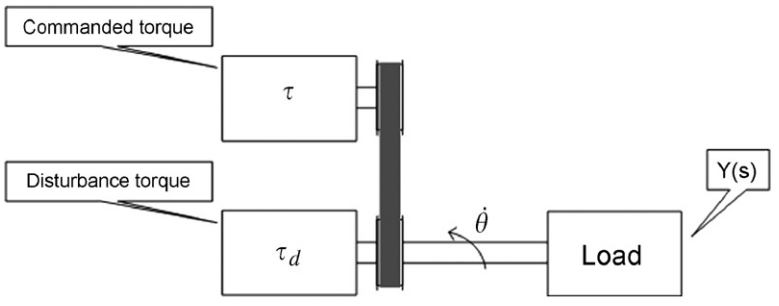

Fig. 1. Typical model of the rotating machine.

where Re denotes the real part of a complex value. The values W and T are phasors defining the amplitude and the phase of each signal for the order n. Eq. (1) can now be rewritten for the order n:

$$W = HT + W_0, \tag{6}$$

where W_0 is the phasor of the shaft speed without active control: $W_0 = HT_d$, $H = Y(\mathrm{j}\omega)$ is the value of the admittance at the frequency ω. That can be also written $H = H_R + \mathrm{i}H_I$ where H_R is the conductance and H_I the susceptance of it. For the special case of Eq. (2), a pure conductance is defined $H = 1/b$ (when $f \ll f_c$) and a pure susceptance is $H = \mathrm{i}I\omega$ (when $f \gg f_c$). In any other case, H is a complex value which varies according to the shaft speed N.

3. Control

3.1. Criterions

The optimal command of the commanded torque is defined as the phasor T that extremalizes a given criterion Q. Different criterions can be proposed, but they can all be defined as a value, J, to maximize or a value, L, to minimize (such as the losses or the cost of the control), or a tradeoff between them:

$$Q(T) = J(T) + L(T). \tag{7}$$

The criterions proposed here are all related to the energy exchanged between the actuator and the mechanical system.

(1) Minimizing the kinetic energy. This is the conventional indicator in active control. At the minimum of this criterion, the phasor W is attenuated. In this case, there is no regard to the control effort or energetical losses. This criterion will always be real positive:

$$Q_1(T) = |W|^2. \tag{8}$$

(2) To maximize mechanical reactive power (i.e. the energy will flow back and forth across the actuator shaft). In this case, the commanded torque acts like a virtual flywheel added to the system. By definition, the reactive power of a mechanical system is the imaginary part of the product between the conjugate of the rotating speed and the torque [14]. Again, no loss tradeoff is considered:

$$Q_2(T) = \mathrm{Im}(WT^*). \tag{9}$$

(3) To minimize mechanical active power. The active power denotes a net variation of energy quantity in the system [14]. When active power is negative, the commanded torque will recuperate energy from the mechanical system and store it in the electrical system. However, it is important to consider losses since the controller has to overcome all heat losses to recuperate energy in electrochemical accumulators or capacitors. The general expression of losses is a function of the torque ($L = \alpha|T|^2$). For example, the losses of an electric direct current motor are created by joule effect: $\alpha = R/2k^2$ where R is the electric motor resistance and k its torque constant [15]. The criterion can then be defined as

$$Q_3(T) = \mathrm{Re}(WT^*) + \alpha|T|^2. \tag{10}$$

3.2. Classical active control

Using Eqs. (6) and (8), the expression of the criterion Q_1, according to T and T_d is

$$Q_1(T) = |H|^2|T + T_d|^2. \tag{11}$$

Obviously, Q_1 is cancelled for $T_{\mathrm{opt}} = -T_d$ whatever the system admittance is. With cancelled speed ripple, the system behaves like a rotating system including a flywheel of infinite mass. Eq. (11) also shows that Q_1 evolves

quadratically according to the torque T, making Q_1 a criterion with only one global extremum. The gradient of Q_1 is expressed as

$$\nabla Q_1 = \frac{\partial Q_1}{\partial T_R} + \mathrm{i}\frac{\partial Q_1}{\partial T_I} = 2H^* W. \tag{12}$$

Eq. (12) shows that when $\nabla Q_1 = 0$, the speed W equals zero. This confirms that the extremum of the criterion Q_1 cancels the kinetic energy.

3.3. Reactive power control

The criterion stated in Eq. (9) can be reformulated according to Eq. (6):

$$Q_2 = \mathrm{Im}(H)|T|^2 + |H||T_d||T|\sin(\angle H + \angle T_d - \angle T). \tag{13}$$

The first part of Eq. (13) is the reactive power due to the mechanical inertia of the system. For the second part it defines the reactive power generated by the commanded torque. Another interesting fact about Q_2 is that it depends on $\angle T$. Then, there is a privileged direction of T where Q_2 reaches its maximum value. Like for Q_1, Q_2 is a quadratic function of T making it a criterion with one global extremum. The optimal commanded torque is then calculated in its polar form by cancelling the gradient of the criterion.

$$\angle T_{\mathrm{opt}} = \angle H + \angle T_d - \frac{\pi}{2} + 2k\pi, \tag{14}$$

$$|T_{\mathrm{opt}}| = \frac{|H|}{2|\mathrm{Im}(H)|}|T_d|. \tag{15}$$

Eqs. (14) and (15) define an optimal matching impedance that ensures the maximal reactive power generated by the actuator (maximization of the energy exchanged between the mechanical system and the actuator during one period). The optimal command depends on the mechanical system dynamics H and the disturbance torque T_d. To obtain a physical sense to that relation, some special cases can be analyzed:

(1) If H is purely real (viscous system without inertia, $\angle H = 0$ rad), it is theoretically possible to maximize the reactive power to infinity as $|T_{\mathrm{opt}}|$ (division by zero) is undefined. The only condition is to have a commanded torque with a $-\pi/2$ phase shift.
(2) If H is purely imaginary (non-viscous system with inertia). In that case, it exists an optimal commanded torque that maximizes the reactive power:

$$T_{\mathrm{opt}} = -\tfrac{1}{2}T_d. \tag{16}$$

3.4. Recuperated active power

As in Section 3.3, the criterion for the recuperated active power (considering the losses) can be rewritten as being:

$$Q_3 = (\mathrm{Re}(H) + \alpha)|T|^2 + |H||T_d||T|\cos(\angle H + \angle T_d - \angle T). \tag{17}$$

When active power is positive, the commanded torque feeds energy to the mechanical system, unlike negative active power which takes away energy from the system. To recuperate this active power in batteries, for example, the losses of the commanded torque source must be overcame. Consequently, $\cos(\angle H + \angle T_d - \angle T)$ must be negative and the second term of Eq. (17) must be superior than the first one. Again, Q_3 evolves quadratically in function of T. This means that the criterion Q_3 has only one global extremum. The optimal command is obtained by cancelling the gradient in its polar form for $Q_3 < 0$, providing the solution:

$$\angle T_{\mathrm{opt}} = \angle H + \angle T_d + \pi + 2k\pi, \tag{18}$$

$$|T_{\text{opt}}| = \frac{|H||T_d|}{2[\text{Re}(H) + \alpha]}. \tag{19}$$

The optimal solution for battery charging depends on the mechanical admittance. It is interesting to remark that less $(\text{Re}(H) + \alpha)$ is, the greater the modulus of the optimal commanded torque. This is easily understandable by the fact that the active energy lost by the mechanical system must be compensated back to it. For example, if the mechanical system is an inertia (the admittance is purely imaginary), the phase of T_{opt} is $\angle T_{\text{opt}} = \angle T_d + \pi/2$ and if $\alpha = 0$, there is no limit on active power "pumped" from the mechanical system. However, due to the losses in the actuator, it exists a tradeoff when $\alpha \neq 0$.

Based on $\angle T_{\text{opt}}$ for Q_2 (Eq. (14)) and Q_3 (Eq. (18)), we find that it is impossible to achieve both energy recuperation and speed ripple cancelation at the same time because the optimal commanded torques to reach each of these goals have an angle of $\pi/2$ apart.

3.5. Method of steepest descent

Because the disturbance torque T_d and the transfer function H can change according to the operating point of the machine, the commanded torque has to be perfectly tuned by the controller. In this paper we propose to use an extremal controller to find the optimal torque T_{opt} by constantly adapting the command to reach the criterion extremum. The method of steepest descent is an iterative algorithm [16]:

$$T_{k+1} = T_k - \mu \nabla Q_n(T_k), \tag{20}$$

where k is the iteration number, μ the converging coefficient that determines the size of each step during the command's adaptation and ∇Q_n the gradient of Q_n that can either be calculated implicitly or explicitly. The implicit calculation uses the theoretical expression of the gradient as a function of H, T and T_d. On the other hand, the explicit control uses commands T in order to identify the gradient without any explicit expression of it.

A block diagram implementing the steepest descent algorithm as an extremal controller is shown in Fig. 2. The commanded torque phasor is generated by the harmonic synthesizer in synchronism with θ according to Eq. (5). The harmonic analyzer reads the instantaneous rotating speed $\dot{\theta}$ in synchronism with θ to extract the phasor W according to Eq. (4). The criterion Q_n is then computed. Its gradient $\hat{\nabla} Q_n$ is estimated by finite difference method. Finally, it is fed to the steepest descent algorithm.

For criterions Q_2 and Q_3, an implicit extremal controller can be theoretically defined. But for those controllers, the torque T_d has to be measured to compute the gradient of the criterions. In practice, the torque measuring devices are too costly to be installed in most systems. So, the explicit control algorithm has to be developed to reach the extremum of Q_2 and Q_3 without a torque sensor.

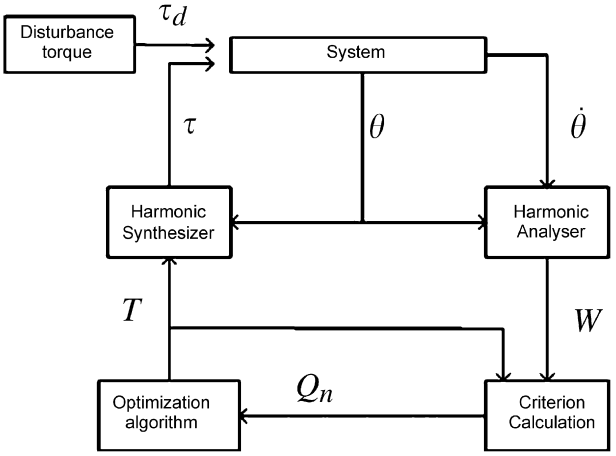

Fig. 2. Block diagram of the extremal controller.

3.5.1. Implicit extremal control

For the minimization of the oscillation, the implicit extremal control of Q_1 can be implemented because $\nabla\hat{Q}_1 = 2H^*W$, hence Eq. (20) becomes

$$T_{k+1} = T_k - 2\mu\hat{H}^*W_k. \tag{21}$$

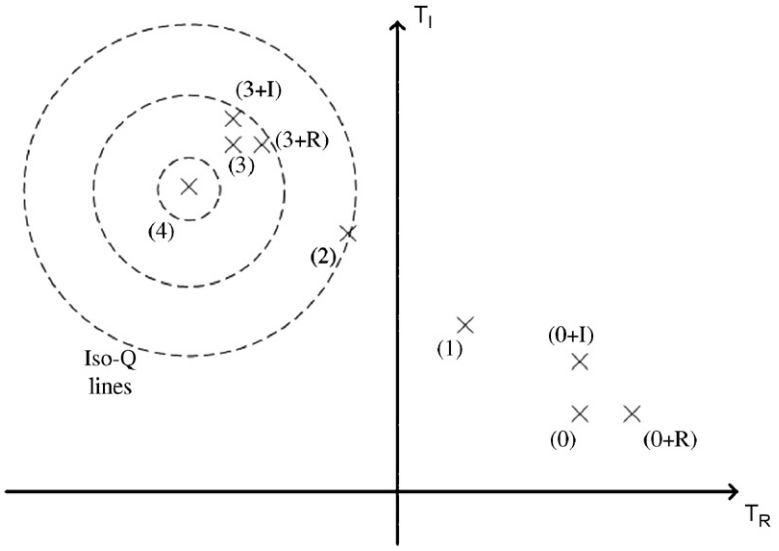

Fig. 3. Graphical representation of the explicit command path.

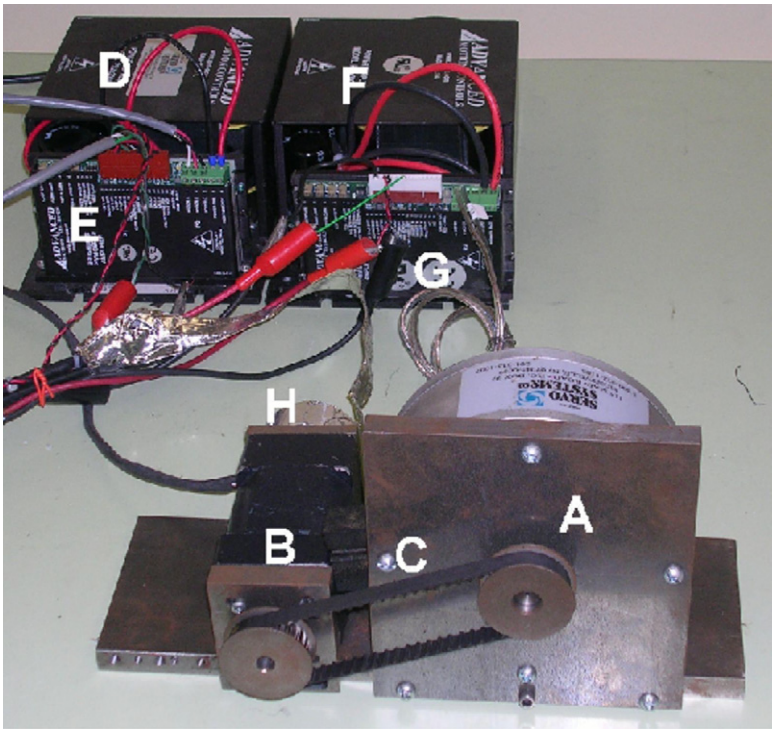

Fig. 4. Test bench picture: (A) direct current machine, (B) permanent magnet synchronous machine, (C) timing belt, (D) power supply for the permanent magnet synchronous machine, (E) permanent magnet synchronous machine current amplifier, (F) power supply for the direct current machine, (G) direct current machine current amplifier and (H) encoder.

The only thing that will impair the performance of this controller is the estimation error between the physical admittance H and its identified value $\hat{H}$. It is well established that if $\angle\hat{H}$ is within $\pm 90^\circ$ of $\angle H$, the controller will still converge to the optimal solution [17]. Only the lapse of time to reach this solution will change according to the identification error. The step factor μ will also have an effect on the convergence of the controller. The optimal step size μ_{opt} is defined as the single step length to jump directly to T_{opt} when $\hat{H} = H$.

$$\mu_{\text{opt}} = \frac{1}{2|H|^2}. \tag{22}$$

So, if $\mu < \mu_{\text{opt}}$ the controller slowly converges to T_{opt}. If $\mu > \mu_{\text{opt}}$, it converges by oscillating around T_{opt}. Finally, if $\mu > 2\mu_{\text{opt}}$ then the controller is unstable and cannot converge. In fact, for a small μ, the controller will converge slowly but retains a good stability. On the other hand, it is possible to accelerate the convergence by increasing μ at the price of a greater chance for the controller to become unstable.

3.6. Explicit extremal control

The idea behind the explicit extremal control is to implement the extremal control of Eq. (20) with an estimation of the gradient when it is impossible to calculate it by sensed signals. The explicit extremal command proceeds by sending small stepped commands to experimentally estimate the gradient. The explicit controller proceeds by executing each of these steps iteratively (please refer to Fig. 3):

(1) Measuring $Q(T)$ (point (0) in Fig. 3).
(2) Sending the command: $T_2 = T + \Delta T_R$, with $\Delta T_R \in \mathbb{R}$.

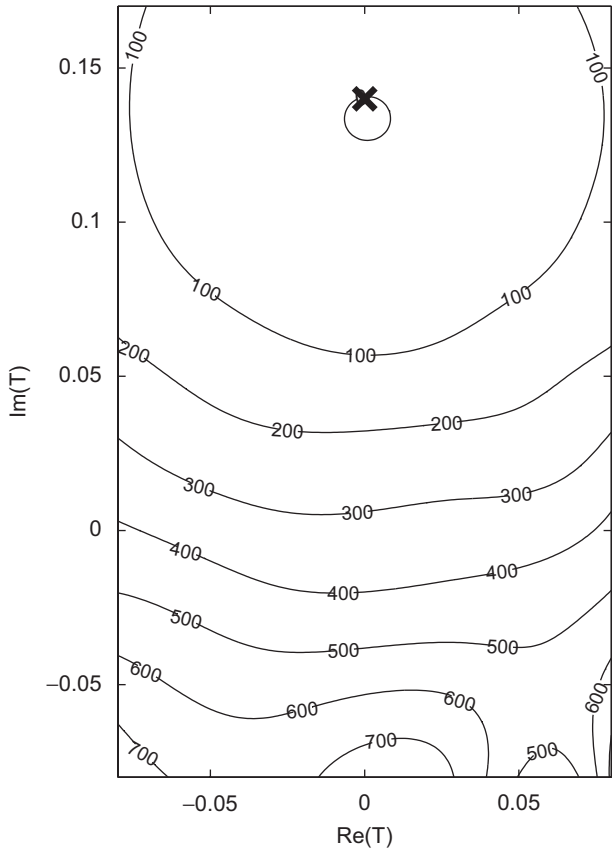

Fig. 5. Speed ripple amplitude versus excitation. $\times T_{\text{opt}}$ theoric, —— Q_1 criterion $(\text{rad/s})^2$.

(3) Measuring $Q(T_2)$ (point $(0+R)$ in Fig. 3).
(4) Calculating $\Delta Q_a = Q(T_2) - Q(T)$.
(5) Sending the command: $T_3 = T + j\Delta T_I$, with $\Delta T_I \in \mathbb{R}$.
(6) Measuring $Q(T_3)$ (point $(0+I)$ in Fig. 3).
(7) Calculating $\Delta Q_b = Q(T_3) - Q(T)$.
(8) Determining the privileged direction $\nabla\hat{Q}(T) = \Delta Q_a/\Delta T_R + \mathrm{j}(\Delta Q_b/\Delta T_I)$.
(9) Stepping forward with the extremal controller algorithm: $T_{k+1} = T_k - \mu\nabla\hat{Q}(T)$ (points (1)–(3) in Fig. 3).

The controller, after estimating the gradient, steps forward in the direction $\nabla\hat{Q}(T)$ until it reaches the minima of the criterion (point (3) in Fig. 3). Once the latter is reached, the controller then recalculates the privileged direction $\Delta\hat{Q}$ (points $(3+R)$ and $(3+I)$ in Fig. 3) and follows it. Each time the direction is recalculated, the step size μ is diminished to make sure that the controller evolves towards the global extremum (point (4) in Fig. 3).

4. Experimental

4.1. Experimental test bench

To verify a practical implementation of the controllers proposed here, an experimental test rig has been developed (Fig. 4). It consists of two torque sources: a direct current machine and a permanent magnet synchronous machine. The direct current machine simulates the disturbance torque of the rotating machine while the permanent magnet synchronous machine is the commanded torque source. Those two motors are

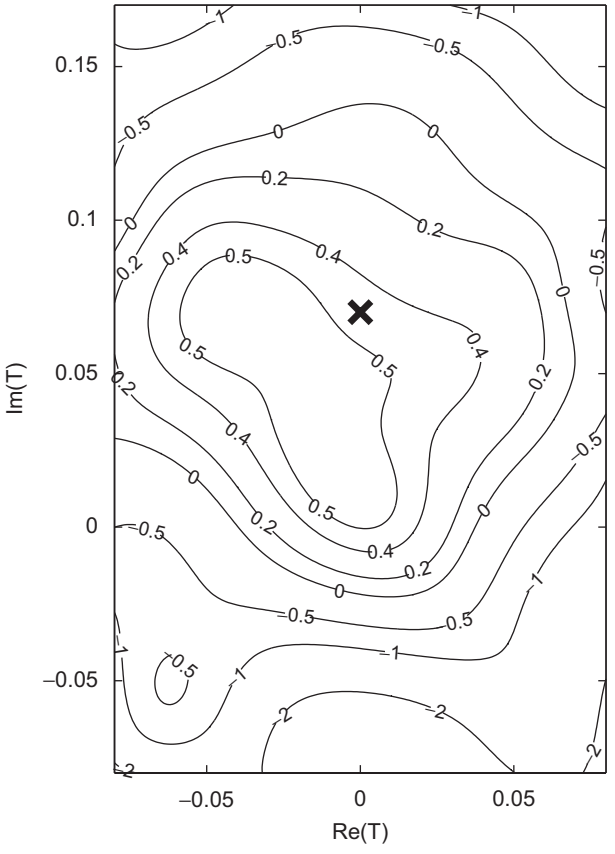

Fig. 6. Reactive power of the permanent magnet synchronous machine versus excitation. $\times T_{\mathrm{opt}}$ theoric, —— Q_2 criterion (W).

coupled together by a timing belt, keeping a 1:1 ratio between them. The timing belt is used to alleviate any risk of slippage between the two torque sources. Both motors are controlled by PWM servo-amplifiers configured in current mode. An encoder with 500 notch/turn and 1 index/turn is used to calculate the speed and the position of the shafts.

To compute the phasor (Eq. (4)), and to generate the command (Eq. (5)) synchronized with the shaft rotation, a reset signal has to be provided each time one period is completed. For this purpose, the index signal of the encoder is connected to an interrupt line of the real time system. The torque signals are acquired by measuring the current monitor pin of each servo-amplifier. Once the speed and torques are measured, it is possible to control the system with the controller. The controller algorithm runs in a dSPACE central

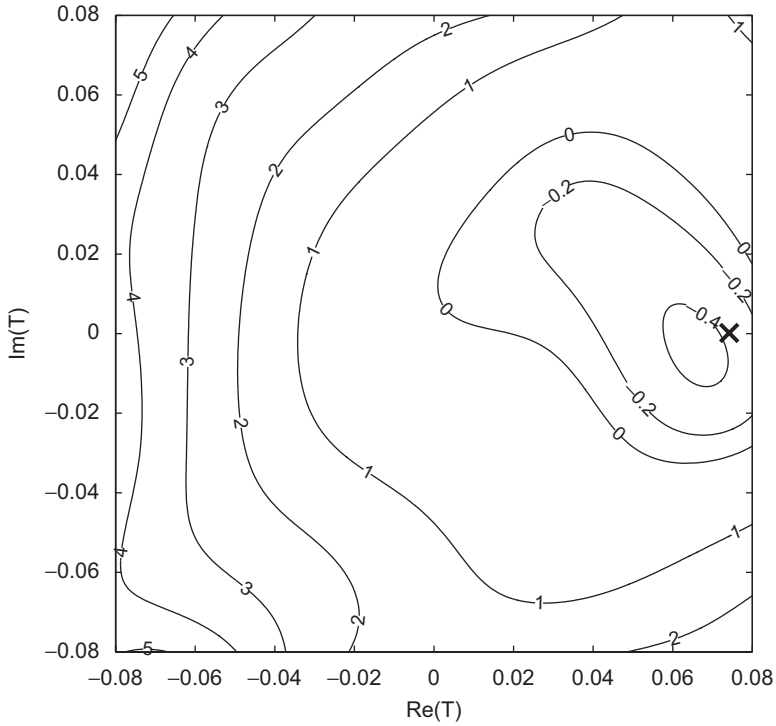

Fig. 7. Total power accumulation versus excitation. $\times T_{\text{opt}}$ theoric, —— Q_3 criterion (W).

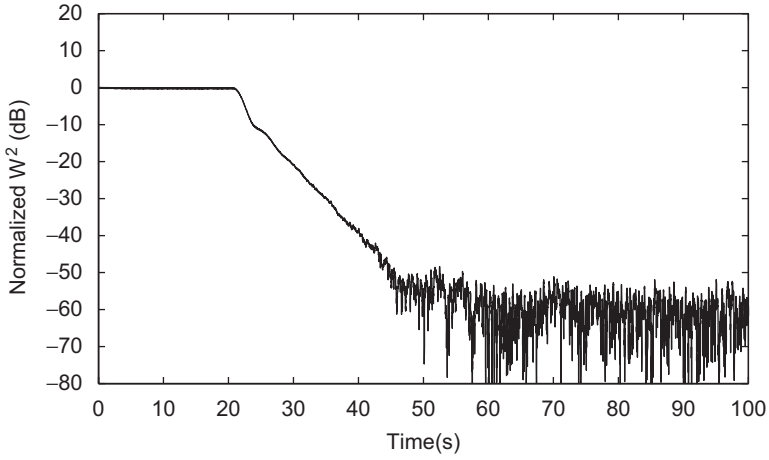

Fig. 8. Criterion to optimize, implicit controller, criterion Q_1.

processing unit. The disturbance torque signal is generated to produce a fluctuating torque at order $n = \frac{1}{2}$, of phasor T_d. The torque signal frequency is half the rotating speed:

$$T_d(\theta) = \mathrm{Re}[T_d e^{i\theta/2}] + D. \tag{23}$$

D is the constant torque added to the disturbance torque. The value of D is determined by a speed controller: a proportional integral controller with a reference speed at 75 rad/s.

4.2. Mechanical admittance

The sampling frequency of the system is set to 100 Hz, allowing enough computational power for rotating speeds between 25 and 150 rad/s. The measured disturbance torque is constant on the test rig for an average speed of 75 rad/s. Its value is $T_d = -0.14i$ N m with a frequency of $\omega = 37.5$ rad/s. The transfer function of the test rig is found by computing the theoretical inertia of the rotating parts ($I = 2.473 \times 10^{-4}$ Kg m^2) and

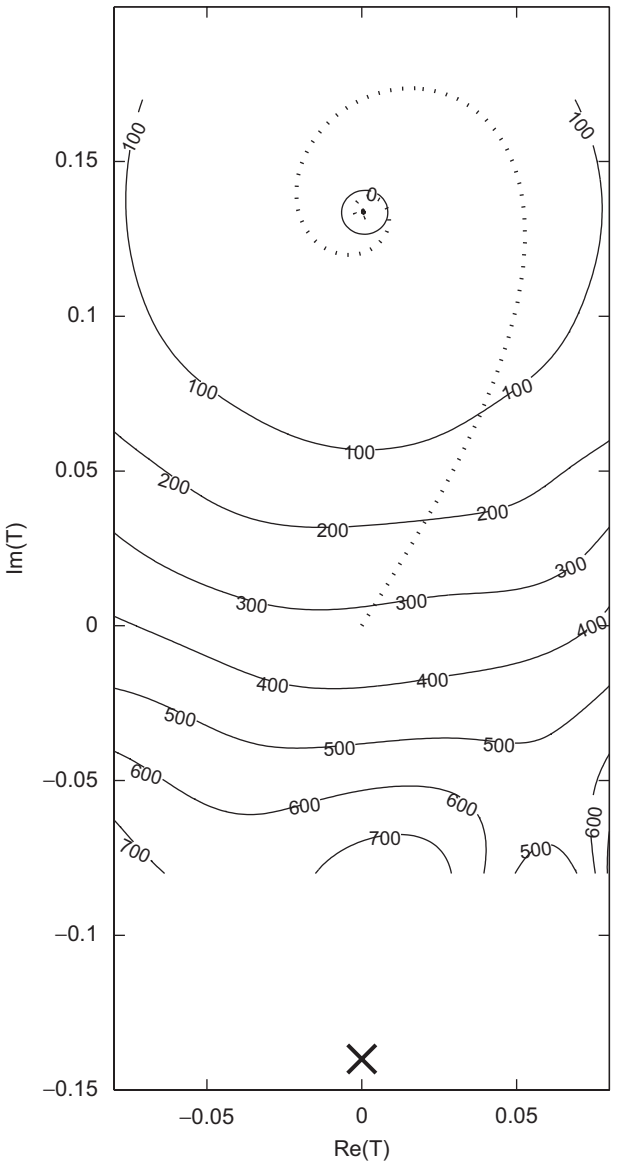

Fig. 9. Controller command path, implicit controller, criterion Q_1. $\times T_c$; —— Q_1 criterion (rad/s)^2, ... controller command.

measuring experimentally the viscous resistance $b = 2 \times 10^{-5}$ N s/m rad. This gives an admittance of $Y(s) = 4044/(s + 0.08087)$ and so $Y(i37.5) = 0.23 - 108i = H$. For this disturbance frequency, the system can be seen as an inertia with negligible viscosity: $H \cong 1/Ij\omega$. This is due to $\omega = 37.5$ rad/s which is very superior to the cutoff frequency $\omega_c = b/I = 0.081$ rad/s.

4.3. Criterion maps

To create the criterion maps of Figs. 5–7, the system rotates with a fluctuating torque given by the direct current machine with an average rotating speed of 75 rad/s. Once the average speed stabilizes, the commanded torque is set to sweep the map area with complex torques of different amplitude and phase. To make the maps, the readings are then extrapolated with Matlab. With the values of the actual disturbance torque and the transfer function, it is also possible to determine the theoric optimal torques for each criterion.

Fig. 5 shows the speed ripple amplitude (criterion Q_1) versus the commanded torque. When $T = 0$, the speed ripple magnitude without active control is close to 400 rad^2/s^2. When the commanded torque reaches the value of the optimal torque $T_{\text{opt}} = -T_d = 0.14i$ N m, the speed ripple magnitude falls to 0, the predicted value of the theoretical expression given by (Eq. (11)).

Fig. 6 shows the reactive power (criterion Q_2) versus the commanded torque. Formulated in Section 3.3, the reactive power is supposed to evolve quadratically according to the commanded torque T. Along with the results of Section 3.3, the optimal torque is $\angle T_{\text{opt}} = \pi/2$ rad, $|T_{\text{opt}}| = 0.07$ N m. Because of a noisy torque signal, the experimental map does not seem to verify the quadratic dependance between T and the reactive power. However, the theoretical optimal command seems to fall near the optimal region of the map, generating an optimal reactive power of 0.5 VAR. This result coincides with the theoretical optimal reactive power of $Q_2 = 0.52$ VAR (Eq. (13)).

Fig. 7 shows the sum of the active power and heat losses versus the commanded torque (criterion Q_3). The optimal torque for criterion Q_3, according to the results of Section 3.4, is $\angle T_{\text{opt}} = 0.0022$ rad, $|T_{\text{opt}}| = 0.0742$ N m. The theoretical optimal torque and experimental extremum meet each other in the map. This map shows that it is possible to recuperate energy (e.g. to charge a battery) with a maximal active power of -0.4 W, compared to a theoretical value of $Q_3 = -0.56$ W (Eq. (17)). As a result, only a small part of the region permits to recuperate energy. Actually, for any commanded torque with $Q_3 > 0$, the battery provide electrical power to the system.

4.4. Optimum command reach

It is important to verify the behavior of each controller proposed in the last section. For this test, once the rotation speed stabilized to the preset value of 75 rad/s, the extremal controller is turned on, and its behavior is

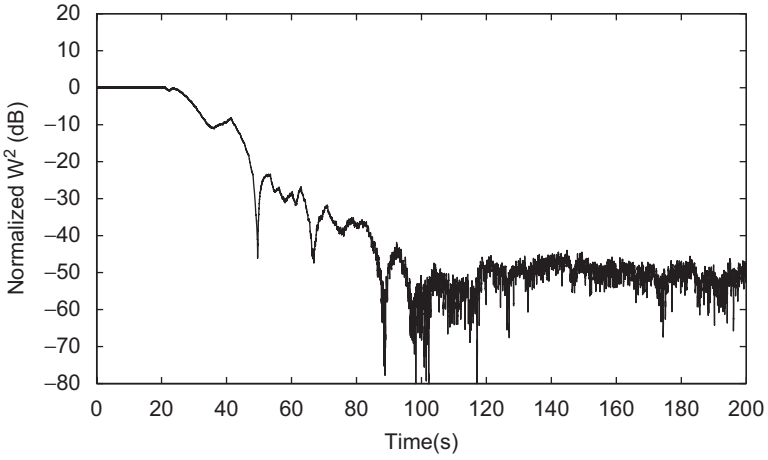

Fig. 10. Criterion to optimize, explicit controller, criterion Q_1.

monitored. Fig. 8 shows the value of the criterion Q_1, minimized by the implicit controller that converges with the path shown in Fig. 9. Fig. 10 shows the same criterion Q_1, but minimized with the explicit controller. The convergence path of this controller is shown in Fig. 11. Since Q_2 can only be maximized by the explicit controller, the value of the criterion is shown in Fig. 12 only, with a converging path described in Fig. 13. For each figure with the controller converging path (Figs. 9, 11 and 13), iso-criterion lines are in the background to help to visualize the trajectory of the controller towards the extremum.

To validate the results obtained with the experimental system, we denote that when minimizing Q_1, the instantaneous speed ripple cancels with both implicit and explicit controllers. We also see that the implicit controller reaches the optimal command quicker (10 s) than the explicit controller (25 s), for about the same attenuation of the speed fluctuations (−45 to −50 dB). For Q_2, the instantaneous speed ripple is attenuated but not as greatly as with Q_1 and the reactive power reaches slowly (50 s) its maximum value (+8 dB). The behavior of each controller is then validated since each of them reaches the extremum of their respective criterion.

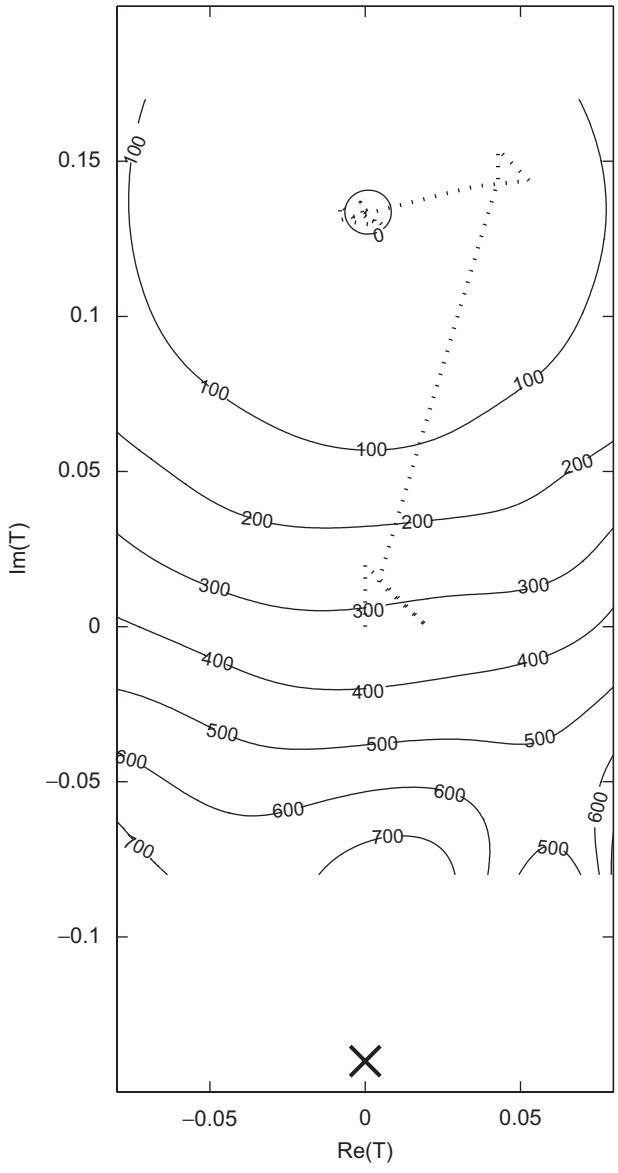

Fig. 11. Controller command path, explicit controller, criterion Q_1. $\times T_c$; — Q_1 criterion $(\mathrm{rad/s})^2$, ... controller command.

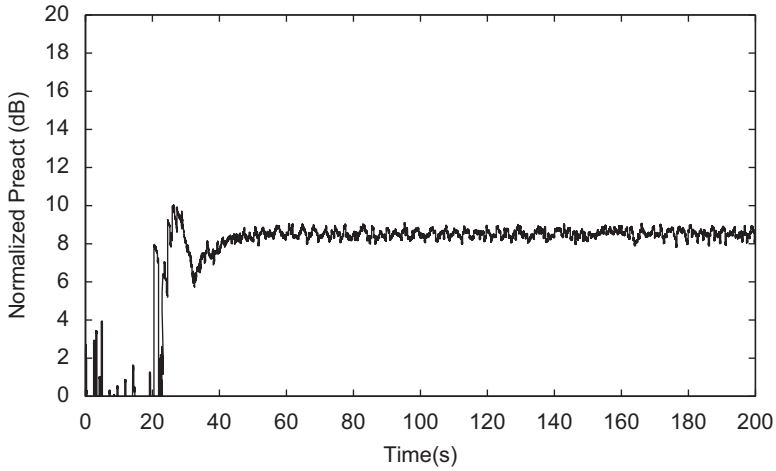

Fig. 12. Criterion to optimize, explicit controller, criterion Q_2.

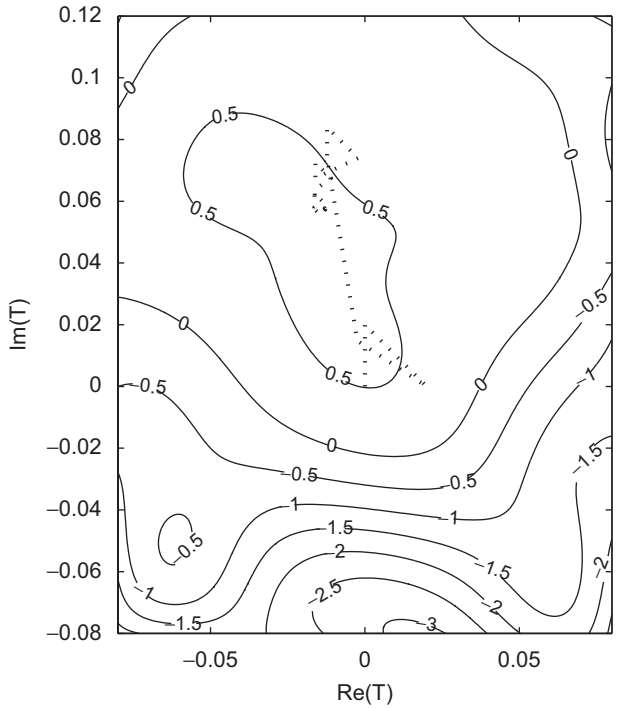

Fig. 13. Controller command path, explicit controller, criterion Q_2. —— Q_2 criterion (W), ... controller command.

5. Conclusion

The proposed controllers all use the extremal command. With the past calculations, it has been determined that the implicit and explicit controllers are possible to realize and will reach the criterions extremum. In the case of reactive and active power, the implicit controller is mathematically possible but it would be not practically achievable. So, for that criterion, only the explicit controller is proposed for an experimental implementation. It has also been proved that all criterions each have one unique extremum which permits the steepest descent algorithm to reach the optimal command. The explicit controller proposed here can be used for any energetic criterion, so it is very useful when it is impossible to calculate the exact gradient. About the meaning of reactive power and active power, those concepts have been explained with regards to power

exchange and the admittance of a mechanical system. It has also been proved that it is possible to do power harvesting with an oscillating torque without drawback on the mean torque because the active anti-torque has an average value of zero according to the shaft angle.

It would be interesting to try this kind of energy harvesting on an electric hybrid vehicle. The disturbance torque would be provided by the combustion engine and the commanded torque would be brought by the motor/generator of the vehicle. The controller would charge the batteries when needed and then, when the batteries are charged, reduces torque ripple only when necessary (during low rev/min operation). The possibility to disable the torque ripple control can permit quicker speed transients of the drivetrain over the traditional flywheel without compromizing comfort. On extreme cases, it would be possible to alleviate the torque ripple totally, like a flywheel of infinite mass would do.

Further experimentations are envisaged on a mechanical system consisting of a one cylinder combustion engine and a permanent magnet electric motor. This system, having a torque ripple made of several dominant harmonics, will be even more near a practical implementation of the controller. It will be interesting to see if the control of torque ripple has an effect on the combustion process of the engine as well.

The controller can be used even for non-rotating systems, as long as the system includes both a force and a speed variable. For example, it could be used to control the vibrations of a structure with piezo-electric sensors and actuators. The sensors would give the speed and the force would be created by the actuators. As the controller is described in this paper, it would work on this kind of system with very minor modifications and is already part of ongoing work.

References

[1] R.I. Davis, A Nonlinear Observer for Instantaneous Internal Combustion Engine Crankshaft Torque and Active Torque Smoothing Control Using a Crankshaft Mounted Electric Motor, PhD Thesis, University of Wisconsin, Madison, 1999.
[2] G. Hillerstrom, On Repetitive Control, PhD Thesis, Lulea University of Technology, 1994.
[3] H. De Battista, R.J. Mantz, Sliding mode control of torque ripple in wind energy conversion systems with slip power recovery, *IECON Proceedings (Industrial Electronics Conference)*, vol. 2, Aachen, Germany, 1998, pp. 651–656.
[4] S.J.E.C.R. Fuller, P.R. Nelson, *Active Control of Vibration*, Academic Press, New York, 1996.
[5] R. Davis, R. Lorenz, Engine torque ripple cancellation with an integrated starter alternator in a hybrid electric vehicle: implementation and control, *IEEE Transactions on Industry Applications* 39 (6) (2003) 1765–1774.
[6] S. Tnani, P. Coirault, G. Champenois, Active flywheel control for hybrid vehicle, *Revue de l'Electricite et de l'Electronique* (1) (2005) 85–90.
[7] Y. Nakajima, M. Uchida, H. Ogane, Y. Kitajima, Study on the reduction of crankshaft rotational vibration velocity by using a motor-generator, *Japan Society of Automotive Engineers Review* 21 (3) (2000) 335–341.
[8] A.T. Zaremba, System for damping engine speed oscillations, US Patent no. 6,286,473 b1, 2000.
[9] A. Zaremba, R. Davis, Control design for active engine damping using a starter/alternator, *Proceedings of the 2000 American Control Conference. ACC (IEEE Cat. No. 00CH36334)*, vol. 3, Chicago, IL, USA, 2000, pp. 2043–2047.
[10] P. Micheau, P. Coireault, A harmonic controller of engine speed oscillations for hybrid vehicles, *Proceedings of the 16th World IFAC Congress, Automotive Control*, Prague, Czech Republic, 2005.
[11] B.M. Badreddine, Active Damping of Engine Idle Speed Oscillation by Applying Adaptive *pid* Control, PhD Thesis, Wayne State University, 2001.
[12] P.M. Morse, *Vibration and Sound*, McGraw-Hill Book Co., New York, 1948.
[13] R.F. Martin, Harmonic currents, Compliance Engineering, 1999 Annual Reference Guide. URL ⟨http://www.ce-mag.com/suppliers/⟩.
[14] Y. Bobrovnitskii, Estimating the vibrational energy characteristics of an elastic structure via the input impedance and mobility, *Journal of Sound and Vibration* 217 (2) (1998) 351–386.
[15] I. Husain, *Electric and Hybrid Vehicles Design Fundamentals*, CRC Press, Boca Raton, FL, 2003.
[16] J.A. Snyman, *Practical Mathematical Optimization: An Introduction to Basic Optimization Theory and Classical and New Gradient-Based Algorithms*, Springer, Berlin, 2005.
[17] J.C.D. Kemin Zhou, *Essentials of Robust Control*, Prentice-Hall, Upper Saddle River, NJ, 1998.